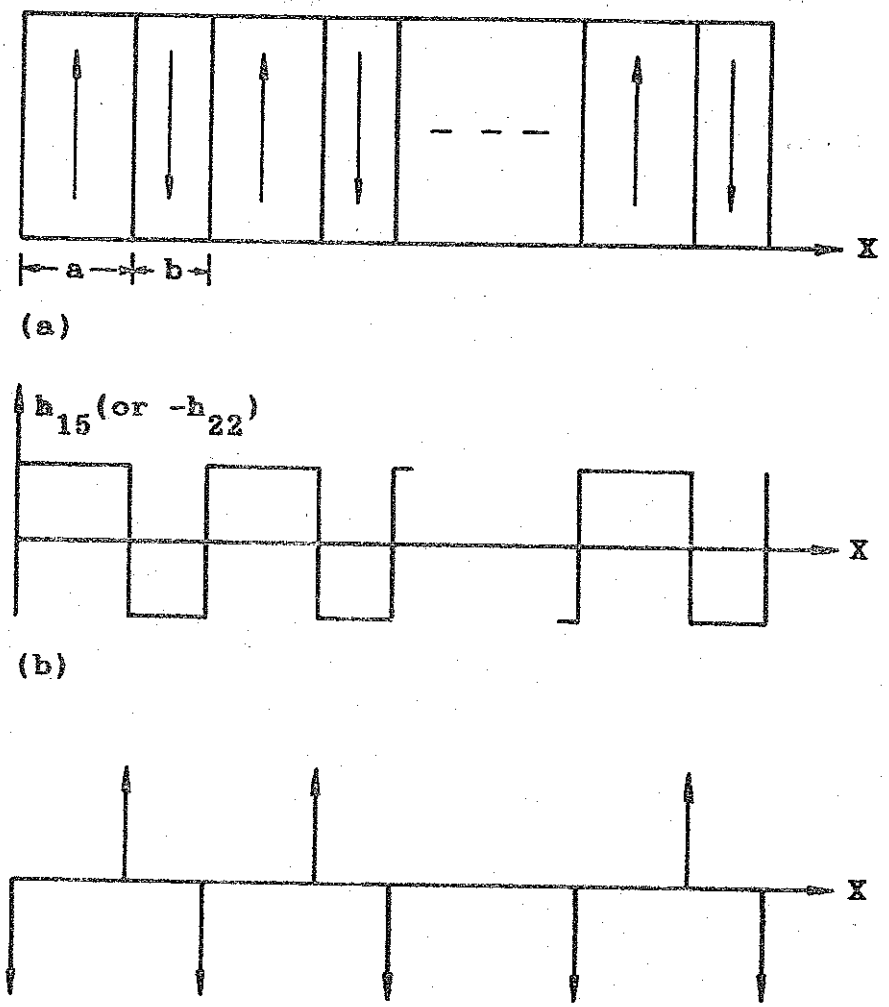

Fig.2—2.ASL of $LiNbO_3$ for excitation of one quasi-longitudinal and one quasi-shear waves. (a)Schematic diagram of ASL (the arrows indicate the directions of the spontaneous polarization). (b)Corresponding piezoelectric coefficient as a periodic function of x. (c)Corresponding sound δ-sources.

acoustic wavelength so that one dimensional model is applicable. Under these conditions, a longitudinal planar

wave propagating along the z axis will be excited by the action of an alternating external electric field. With $\partial/\partial x=\partial/\partial y=0$, the piezoelectric equations[4] relative to this case are

$$T_3=C_{33}^{D}S_3+(-1)^{n}h_{33}D_3 \quad , \tag{2—1}$$

$$E_3=(-1)^{n}h_{33}S_3+(\varepsilon_{33}^{s})^{-1}D_3 \quad , \tag{2—2}$$

$n=1,2,3,\ldots,2N$.

Where T_3, S_3, E_3, D_3 are the stress, strain, electric field, electric displacement, respectively. C_{33}^{D}, h_{33}, ε_{33}^{s} are the elastic, piezoelectric, dielectric coefficients, respectively. And the Newton's motion equation is

$$\partial T_3/\partial z=\rho\partial^2 U_3/\partial t^2, \tag{2—3}$$

here ρ represents the density, U_3 the particle displacement from equilibrium position in the z direction.

Differentiating Eq.(2—1) twice with respect to time and Eq.(2—3) once with respect to z we obtain

$$\partial^2 T_3/\partial t^2=C_{33}^{D}\partial^3 U_3/\partial t^2\partial z+(-1)^{n}h_{33}\partial^2 D_3/\partial t^2, \tag{2—4}$$

$$\rho\partial^3 U_3/\partial z\partial t^2=\partial^2 T_3/\partial z^2. \tag{2—5}$$

By reversing the order of differentiation we can substitute Eq.(2—4) into Eq.(2—5) and obtain

$$\partial^2 T_3/\partial t^2-(C_{33}^D/\rho)\partial^2 T_3/\partial z^2=(-1)^n h_{33}\partial^2 D_3/\partial t^2. \qquad (2—6)$$

This is the fundamental wave equation governing the excitation and propagation of stress in a piezoelectric ASL. The presence of the term on the right-hand side makes it an inhomogeneous equation. It is this term which describes the excitation of the waves while the homogeneous left-hand side describes their propagation.

If we assume that all variables have the same time dependence $\exp(j\omega t)$, then Eq.(2—6) becomes

$$\partial^2 T_3/\partial z^2+k^2 T_3=(-1)^n h_{33}k^2 D_3, \qquad (2—7)$$

where $k=\omega/v$ is the wave vector, $v=\sqrt{C_{33}^D/\rho}$, represents the sound velocity.

We will use the Green's function method[4] to solve the wave equation. In order to satisfy the free boundary condition, a particular technique must be used which is the so-called the "method of images". The method consists in noting that homogeneous boundary conditions can be satisfied along a plane boundary by introducing one fictitious "image source" for every real source. This image source is of opposite polarity if zero T_3 is required on the boundary. It is placed on the opposite side of the boundary plane and the same distance from the boundary as the real source(Fig.2—3). Physically, this is equivalent to treating the waves reflected by the boundary as the waves emitted by the "image sources". The boundary may now be forgotten and the solution obtained merely by analyzing the effects of the real and imaging sources. The solution is valid only on the

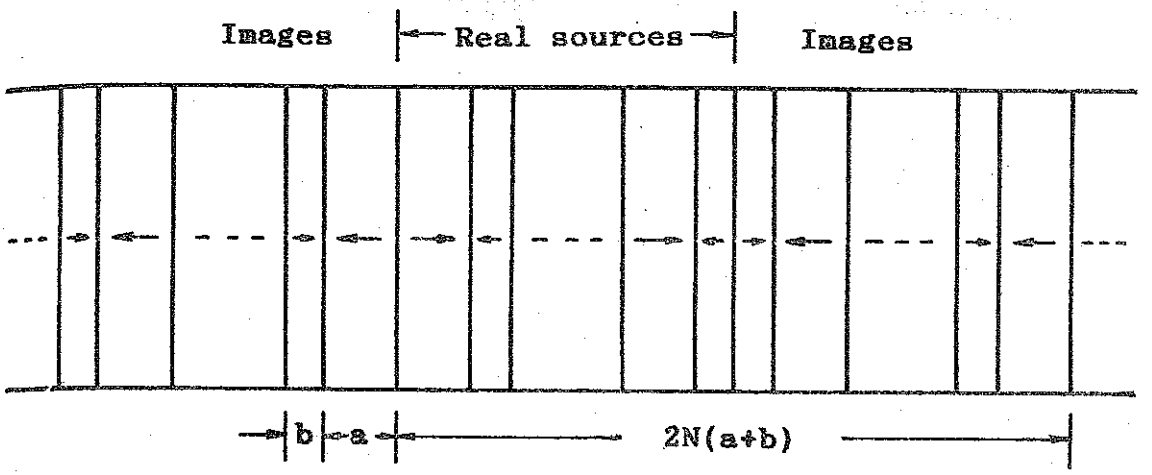

Fig.2—3.ASL with its images. A long periodicity, 2N(a+b), appears.

"real" side of the boundary, of course.

The method of images makes heavy use of the Green's function for boundaries at infinity. In our case, the Green's function for one dimension is

$$G(z',z)=(-j/2k)\exp(-jk|z'-z|), \qquad (2—8)$$

here z' and z are the positions of sound source and observation, respectively.

According to the Green's function method,the stress at a point within the ASL is the sum of the stress waves generated from sound source points, including images, on both sides. It can be expressed as[4]

$$T_3(z)=-(1/2)jk\{\exp(-jkz)F(h_{33}D_3)$$

$$-2j\int_{z}^{\infty} h_{33}(z')D_3(z')\sin\left[k(z'-z)\right]dz'\Big\}. \qquad (2-9)$$

Where h_{33} and D_3 include both real-source and image-source distributions, and $F(h_{33}D_3)$ is

$$F(h_{33}D_3)=h_{33}D_3\int_{-\infty}^{\infty} f(z)e^{jkz}dz. \qquad (2-10)$$

Where

$$f(z)=\begin{cases} +1, & \text{if } z \text{ is in the positive domains,} \\ -1, & \text{if } z \text{ is in the negative domains.} \end{cases}$$

In order to understand the electrical properties of the ASL. we need to know its impedance which expresses the relationship between applied voltage(V) and electric current(I). Here

$$-V=\int E_3 dz, \qquad (2-11)$$

$$I=j\omega A_{12}D_3 , \qquad (2-12)$$

here A_{12} is the electrode area,ω is the angular frequency.

From now on, we will discuss two different boundary conditions, one for resonators and the other for transducers.

A.Resonators

The boundary conditions are

$$T_3(z=0)=T_3[\,z=N(a+b)]=0. \qquad (2\text{—}13)$$

Under these conditions,the images must be introduced repeatedly in order to satisfy the stress-free boundary conditions on both electrode faces. In doing so, a longer periodicity, 2N(a+b), is superimposed on the original ASL as shown in Fig.(2—3). Using the Green's function method, we get the stress in the positive domains

$$T_3^P=h_{33}D_3+T, \qquad (2\text{—}14)$$

and the stress in the negative domains

$$T_3^n=h_{33}D_3\left\{-1+2\cos\left[k(z-(n+1)a-nb)\right]\right\}+T. \qquad (2\text{—}15)$$

Here

$$T=h_{33}D_3\left\{-4\sin\left(\frac{1}{2}kb\right)\frac{\sin\left\{\frac{1}{2}kn(a+b)\right\}}{\sin\left\{\frac{1}{2}k(a+b)\right\}}\sin\left\{k\left[z-\frac{1}{2}(n+1)a-\frac{1}{2}nb\right]\right\}\right.$$

$$-\frac{\cos\left\{\frac{1}{2}k\left[(N-1)a+(N+1)b\right]\right\}}{\cos\left[\frac{1}{2}kN(a+b)\right]\sin\left[\frac{1}{2}k(a+b)\right]}\sin(kz)$$

$$\left.+\frac{\sin k\left[z-\frac{1}{2}(a+b)\right]}{\sin\left[\frac{1}{2}k(a+b)\right]}\right\}. \qquad (2\text{—}16)$$

Also we get the impedance of the ASL

$$Z=\left[\frac{2h_{33}^{2}v}{j\omega^{2}A_{12}C_{33}^{D}}\right]\left\{-4N\frac{\sin(\frac{1}{2}ka)\sin(\frac{1}{2}kb)}{\sin\frac{1}{2}k(a+b)}\right.$$

$$\left.-\frac{\sin^{2}[\frac{1}{2}k(a-b)]}{\sin^{2}[\frac{1}{2}k(a+b)]}\tan[\frac{1}{2}kN(a+b)]\right\}+\frac{N(a+b)}{j\omega A_{12}\varepsilon_{33}^{s}}\ . \qquad (2—17)$$

From Eq.(2—17), following conclusions can be derived.

The resonances occur when $Z\rightarrow\infty$. There exist two different cases.

Firstly, let $\sin[k(a+b)/2]=0$, we have

$$f_{main}^{n}=v/(a+b),\ n=1,2,3,\ldots\ . \qquad (2—18)$$

Here we call f_{main}^{n} the main resonance(MR) frequency and f_{main}^{1} is the fundamental frequency of the MRs. The fact that the MRs are determined only by the periodicity of the ASL, a+b, not by its total thickness is of great practical significance. As we know, the thickness of a resonator working at hundreds megahertz with ordinary materials, such as the single domain $LiNbO_3$ crystal, is several microns or tens of microns, which is too thin to be fabricated by ordinary processing techniques. However, according to Eq.(2—18), we can see clearly that the thinner the laminar domains, the higher the resonance frequencies. In practice, a thickness of laminar domains of several microns can be achieved, which corresponds to the resonance frequencies of hundreds megahertz to several gigahertz. Therefore, it is possible to fabricate the acoustic devices operating at very

high frequencies by using the ASL.

Secondly, let $\tan[kN(a+b)/2] \longrightarrow \infty$ and take f^1_{main} for the reference frequency, then we have

$$f^m_s = mv/[2N(a+b)] = mf^1_{main}/2N, \quad m=\pm1,\pm3,\pm5,\ldots . \qquad (2\text{—}19)$$

We call f^m_s the satellite-like resonance(SLR) frequency which locates on either side of the main one and is related to the total thickness of the ASL, N(a+b) only.

The frequency difference between any two adjacent SLRs is given by

$$\Delta f_s = f^{m+2}_s - f^m_s = f^1_{main}/N, \qquad (2\text{—}20)$$

which is just one-Nth of f^1_{main}.

If the thicknesses of positive domains and negative domains are equal, i.e., a=b, Eq.(2—17) can be simplified to

$$Z = \frac{2Na}{j\omega A_{12}\varepsilon^s_{33}} \left\{ 1 - \frac{h^2_{33}\varepsilon^s_{33}}{C^D_{33}} \frac{\tan(\frac{1}{2}ka)}{\frac{1}{2}ka} \right\} . \qquad (2\text{—}21)$$

In this case there exist only main resonances, no satellite-like ones. Here as we know, in solving the wave equation by using the Green's function method, the image sources must be introduced in order to satisfy the free boundary conditions at both electrodes. Thus a longer periodicity, 2N(a+b), is superimposed on the original ASL. Nevertheless, when a=b, the longer periodicity does not

appear. This phenomenon is similar to that in x-ray or electron diffraction. This common feature originates from the common nature of the three interaction systems. First, the acoustic wave, x-ray and electron can all be treated as waves. Second, the media involved in the interaction processes all possess super-structures.

If a=0 (or b=0),Eq.(2—17) can be reduced to

$$Z=\frac{L}{j\omega A_{12}\varepsilon^{s}_{33}}\left\{1-\frac{h^{2}_{33}\varepsilon^{s}_{33}}{C^{D}_{33}}\frac{\tan(\frac{1}{2}kL)}{\frac{1}{2}kL}\right\}. \qquad (2—22)$$

It is the same as that of a resonator made of a single domain $LiNbO_3$ crystal with thickness equal to L (L=Nb or Na)[5].

Comparison Eq.(2—21) with Eq.(2—22) shows that Eq.(2—21) is equivalent to the one for a system made up of 2N identical piezoelectric resonators connected in series, the thickness of each is a. To explain this, we must resort to Eqs.(2—14) and (2—15). We find that, under the stress-free boundary conditions here, the stress on the domain walls are also equal to zero. That is to say, the ASL can be considered to be composed of 2N individual crystal plates each oscillates independently. However, this simplification is not shared by the situation when a is not equal to b.

B.Transducers

The boundary conditions are

$$T_3(z=0)=T_3(z\longrightarrow\infty)=0, \qquad (2\text{—}23)$$

i.e., one face is free and the other face is fully matched to a semi-infinite transmission medium. Here, like the ASL, the transmission medium is also a $LiNbO_3$ crystal but with single domain. Using the same analysis we have obtained

$$Z=R-jX,$$

$$R=\frac{4h_{33}^2 v}{\omega^2 C_{33}^D A_{12}}\left\{\frac{\sin[\frac{1}{2}kN(a+b)]}{\sin[\frac{1}{2}k(a+b)]}\right\}^2$$

$$\times\left\{\left[\cos[\tfrac{1}{2}k(a-b)]-\cos[\tfrac{1}{2}k(a+b)]\right]\cos[\tfrac{1}{2}kN(a+b)]\right.$$

$$\left.-\sin[\tfrac{1}{2}k(a-b)]\sin[\tfrac{1}{2}kN(a+b)]\right\}^2,$$

$$X=\frac{4h_{33}^2 v}{\omega^2 C_{33}^D A_{12}}\left\{\frac{\sin[\frac{1}{2}kN(a+b)]}{\sin[\frac{1}{2}k(a+b)]}\right\}^2$$

$$\times\left\{\left[\cos[\tfrac{1}{2}k(a-b)]-\cos[\tfrac{1}{2}k(a+b)]\right]\cos[\tfrac{1}{2}kN(a+b)]\right.$$

$$\left.-\sin[\tfrac{1}{2}k(a-b)]\sin[\tfrac{1}{2}kN(a+b)]\right\}$$

$$\times\left\{\left[\cos[\tfrac{1}{2}k(a-b)]-\cos[\tfrac{1}{2}k(a+b)]\right]\sin[\tfrac{1}{2}kN(a+b)]\right.$$

$$+\sin\left[\frac{1}{2}k(a-b)\right]\cos\left[\frac{1}{2}kN(a+b)\right]\Bigg\}$$

$$+\frac{h_{33}^{2v}}{\omega^2 C_{33}^{D} A_{12}}\left\{4N\cot\left[\frac{1}{2}k(a+b)\right]-4N\frac{\cos\left[\frac{1}{2}k(a-b)\right]}{\sin\left[\frac{1}{2}k(a+b)\right]}\right.$$

$$\left.-\left[3-2\cos(ka)-2\cos(kb)+\cos\left[k(a+b)\right]\right]\frac{\sin[kN(a+b)]}{2\sin^2\left[\frac{1}{2}k(a+b)\right]}\right\}$$

$$+\frac{N(a+b)}{\omega A_{12}\varepsilon_{33}^{s}}. \qquad (2—24)$$

The resonance frequency, i.e., the operating frequency of the transducer we are interested in, can be obtained by setting $\sin[k(a+b)/2]=0$ which is the same as the MR of the resonator. The difference here is no SLR exists. This is due to our assumption that the transducer is fully matched to a semi-infinite transmission medium. By the use of image method, no longer periodicity has been introduced, so no satellite-like resonance exists.

If a=b, Eq.(2—24) can be reduced to

$$R=\frac{h_{33}^{2v}}{\omega^2 C_{33}^{D} A_{12}}\tan^2\left[\frac{1}{2}ka\right]\sin^2 2Nka,$$

$$X=\frac{h_{33}^2}{\omega^2 C_{33}^D A_{12}}\left\{4N+\frac{1}{2}\tan\left(\frac{1}{2}ka\right)\sin(4Nka)\right\}\tan\left(\frac{1}{2}ka\right)+\frac{N(a+b)}{\omega A_{12}\varepsilon_{33}^s}\,. \tag{2—25}$$

This expression is much the same as one for interdigital transducers derived by equivalent circuit method[6]. The difference is due to the fact that in our case, one face of the transducer(z=0) is stress-free, whereas the interdigital transducer is fully matched to the medium on both sides.

From Eqs.(2—24) and (2—25) we can see that Z is a function of N and A_{12}, hence R and X can be regulated by an adequate choice of the values of N and A_{12}. For transducers made of z-cut single domain $LiNbO_3$ crystals with an electromechanical coupling constant K=0.17, under high frequency operation the static capacitance is the main part of the impedance at resonance frequency. As a result, the insertion loss of the transducer is very high[7]. In our case, however, R can be equal to or even larger than X by choosing N and A_{12} suitably. For example, in the special case of a=b, at the fundamental resonance frequency $f_{main}^1=v/2a$, Eq.(2—25) can be simplified to

$$Z=R-jX=\frac{1}{2\pi f_{main}^1 C_0}\left(8NK^2/\pi-j\right)\,, \tag{2—26}$$

here $C_o=\varepsilon_{33}^s A_{12}/2Na$ is the clamped capacitance. Let $A_{12}=5.0mm^2$, N=15 and a=6.6μm, then R=50Ω, X=45Ω at $f_{main}^1=554MHz$. The transducers thus fabricated will have an insertion loss very low in a 50Ω measurement system. As for the case of a≠b, from Eq.(2—24) we can show that the real

part of the impedance will decrease with the difference between a and b. For example, we consider the situation when the transducer is at its fundamental frequency, i.e., $k(a+b)/2=\pi$. Then Eq.(2—24) reduces to

$$R=\frac{4h_{33}^2N^2v}{\omega^2C_{33}^DA_{12}}\left[\cos\left[\frac{1}{2}k(a-b)\right]+1\right]^2, \tag{2—27}$$

If a=b, we have

$$R=\frac{16h_{33}^2N^2v}{\omega^2C_{33}^DA_{12}}. \tag{2—28}$$

But if b=2a, we have $(\frac{1}{2}ka=\pi/3)$

$$R=\frac{9h_{33}^2N^2v}{\omega^2C_{33}^DA_{12}}. \tag{2—29}$$

Thus we can see that the inequality of the thicknesses of the positive and the negative domains decreases the resistance greatly.

In the limiting case, i.e., when N=1 and b=0 (or a=0), Eq.(2—24) reduces to the normal formula for transducers made of single domain $LiNbO_3$ crystals[5].

If the normal of the laminar domain walls does not coincide with the z axis, but lies in the yz plane, and the electrodes of the transducer are still made parallel to the lamellae of the ASL, then one quasi-longitudinal wave(QLW)

and one quasi-shear wave(QSW) will be generated by the transducer[8]. In such a case, theoretical analysis has shown (see Appendix) that the electrical impedance Z consists of two parts, one for QLW and the other for QSW. The expression for the resonance frequency, Eq.(2—18), still holds except for the substitution of v_L (or v_S) for v, i.e.,

$$f_n^{L(S)}=nv_{L(S)}/(a+b),n=1,2,3,\ldots, \qquad (2—30)$$

here $v_{L(S)}$ is the sound velocity of QLW(QSW).

Under more general condition, i.e., the normal of the walls is along an arbitrary direction, there will be three waves excited, one QLW and two QSWs. This situation will not be treated here.

§2--2.Experimental results

A.Electrical measurements for resonators

The crystals with an ASL used were grown along the z axis. A set of resonators have been made ranging from 500 MHz to 1000 MHz. The periodicity of the ASL inside the resonators is along the z axis perpendicular to the lamellae and the two electrodes are the xy planes parallel to the lamellae. Under the action of an external periodic electric field, an acoustic wave is excited inside the resonator through the piezoelectric effect and it will form a stationary wave when Eqs.(2—18) or (2—19) is satisfied.

With an Hp 8505 network analyzer we have measured the reflection coefficients of the resonators. Its principle is as follows. As we know, if the impedance of a load is not

equal to that of the electric measurement system, the electric energy will be reflected by the load. When a resonator is in oscillation, its impedance will vary with frequency. At the vicinity of the resonance, the impedance of the resonator changes greatly. This will be reflected in the reflection coefficient.That is,the reflection coefficient will approach its minimum. Fig.2—4 shows the result of resonator No.5. In Fig.2—4, curve A represents the frequency dependence of the phase of the reflection coefficient, curve B the frequency dependence of the magnitude. Near the resonance frequency 552MHz, both the phase and the magnitude of the reflection coefficient vary

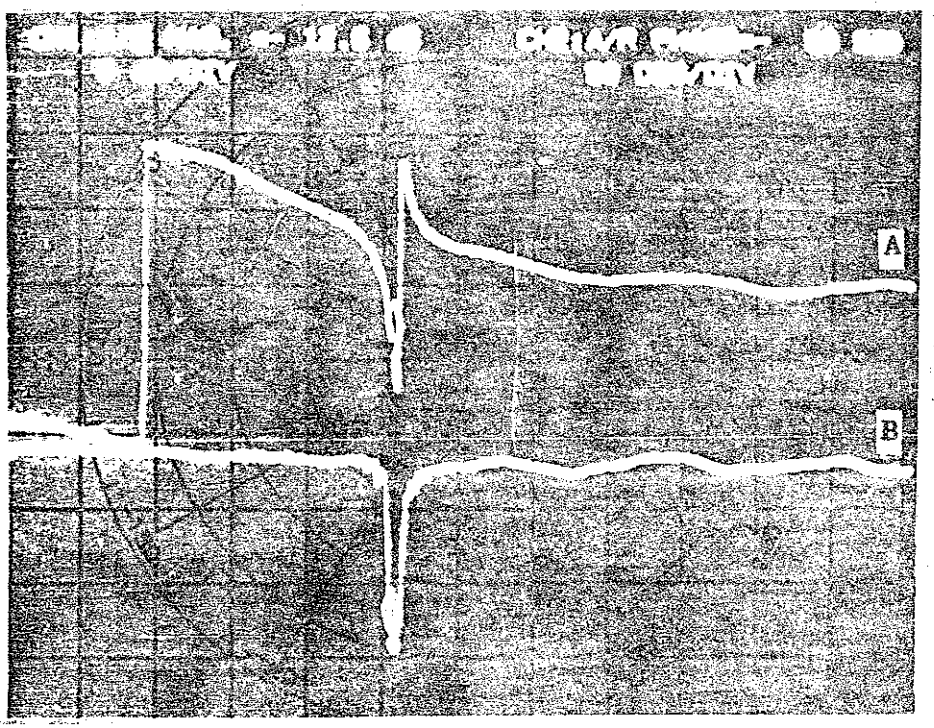

Fig.2—4.Reflection coefficient of the resonator No.5 in rectangular coordinates. The horizontal scale is frequency centered at 650 MHz with scan width f=1300MHz, curve A for phase and curve B for magnitude.

markedly. It can be seen that there is only one MR in the range of 0—1300 MHz, which is conformed to the theory. The resonance frequency is 552 MHz, close to the theoretical value, 554 MHz, which is calculated from Eq.(2—18) with a+b=13.2μm and v=7320m/s for resonator No.5. The measured

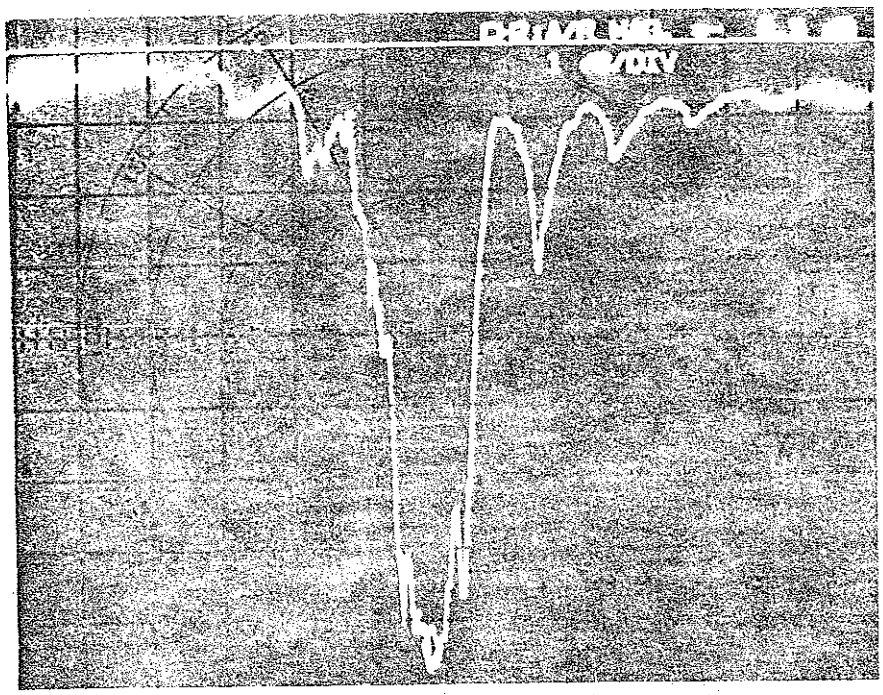

Fig.2—5.Magnitude of the reflection coefficient of the resonator No.6 in rectangular coordinates. The horizontal scale is frequency centered at 553 MHz with scan width f=200 MHz.

and calculated resonance frequencies are listed in table 2—1. It may be noted that the experimental values are very close to the theoretical ones.

Fig.(2—5) has manifested that there do exist a series of satellite-like resonances located on both sides of the

Table 2—1.Relationship between the MR frequency f^1_{main} and the periodicity of ASL for resonators

Resonator	Thickness of positive domain a (μm)	Thickness of negative domain b (μm)	Periodicity of ASL a+b (μm)	Frequency of MAR f^1_{main} (MHz)	
				cal.	meas.
No.1	2.8	4.6	7.4	989	975
No.2	2.0	6.2	8.2	892	882
No.3	4.0	6.0	10.0	732	710
No.4	5.4	5.6	11.0	665	686
No.5	6.2	7.0	13.2	554	552
No.6	5.7	7.6	13.3	550	553

Table 2—2. Frequency difference between any two adjacent SLRs for resonator No.6 made of ASL, $\Delta f_s = f_s^{m+2} - f_s^m$.

	m	1	3	5	7	9
	f_s^m	560.3	577.9	595.1	612.4	629.6
Δf_s (MHz) (measured values)	Δf_s	17.6	17.2	17.3	17.2	
	$\overline{\Delta f_s}$	17.3				

	N	32
$\Delta f_s = f_{main}^1/N$ (theoretical values)	a+b	13.3 μm
	v	7320m/s
	f_{main}^1	550
(MHZ)	Δf_s	17.2

main resonance. Up to our knowledge, before our work, there is no such phenomenon observed in resonators. Note that the thicknesses of the positive domains and the negative domains of the sample used are not equal. This is just predicted by the theory. Table 2—2 shows that the measured frequency difference between any two adjacent SLRs, $\overline{\Delta f}_s$ is in good agreement with the theoretical one calculated from Eq.(2—20).

B.Electrical measurements for transducers

Transducers have been made of the ASL. Here the growth direction of the crystal deviates from the z axis and lies in the yz plane. Therefore the normals of the laminar domain walls of the ASL are not parallel to the z axis. The angles between the normals and the z axis are shown in table 2—3. The two electrodes are both parallel to the lamellae. Each transducer is indium bonded to the xy plane of a single domain $LiNbO_3$ sample separately. The sample, as a transmission medium, has its faces polished flat to about one-tenth of a light wavelength used for examining the sample, and parallel to each other within several minutes. The length of the samples is 3.0mm and the dimensions of the electrodes are about $5.0mm^2$.

In order to evaluate the performance of the transducers, both frequency domain and time domain measurements are made.

In frequency domain measurements, an Hp 8505 network analyzer has been used. We measured the reflection coefficients of the transducers. A typical one is shown in

Fig.2—6. Two resonance frequencies are observed. One is for QLW and the other for QSW with frequencies of 555 MHz and 279 MHz, respectively. Theoretical values, calculated from Eq.(2—30) with a+b=13.2 μm, v_L=7300m/s and v_S=3600m/s[9], are 553 MHz for QLW and 273 MHz for QSW. Table 2—3 lists the resonance frequencies measured and calculated. Obviously the theoretical and experimental results are satisfactory.

So far as the transducer is concerned, the insertion loss is a very important parameter. According to Sittig[10], the insertion loss (IL) of a transducer can be expressed as

$$IL=2(ML+DL), \qquad (2—31)$$

here ML is the "matching loss" and DL the "dissipation loss" which measures the acoustic power absorbed in the transducer due to internal dissipation from dielectric, sound absorption and other losses. In transducers made of single domain $LiNbO_3$ crystals, experiments showed that DL<<ML[10], so that the transducer loss and its dependence on frequency is mainly determined by ML. Here, in order to estimate the insertion loss, as a rough approximation, we neglect the dissipation loss, then we have[10]

$$IL=-20\log(1-r^2), \qquad (2—32)$$

here r is the modulus of the reflection coefficient. With Eq.(2—32), we have calculated the insertion loss versus frequency for transducer No.1 from the measured value of r. The results is shown in Fig.2—7. The insertion loss at 555

Table 2—3. Comparison between theoretical predictions and experimental results for transducers made of ASL.

Transducer	Periodicity of super-lattice a+b (μm)	Number of periods N	Angle between normal of domain boundaries and Z axis(degrees)	Resonance frequency of QLW(MHz) cal.	meas.	Resonance frequency of QSW(MHz) cal.	meas.
#1	13.2	15	5	553	555	273	279
#2	10.8	55	50	648	641	383	380
#3	9.6	62	30	750	764	415	418

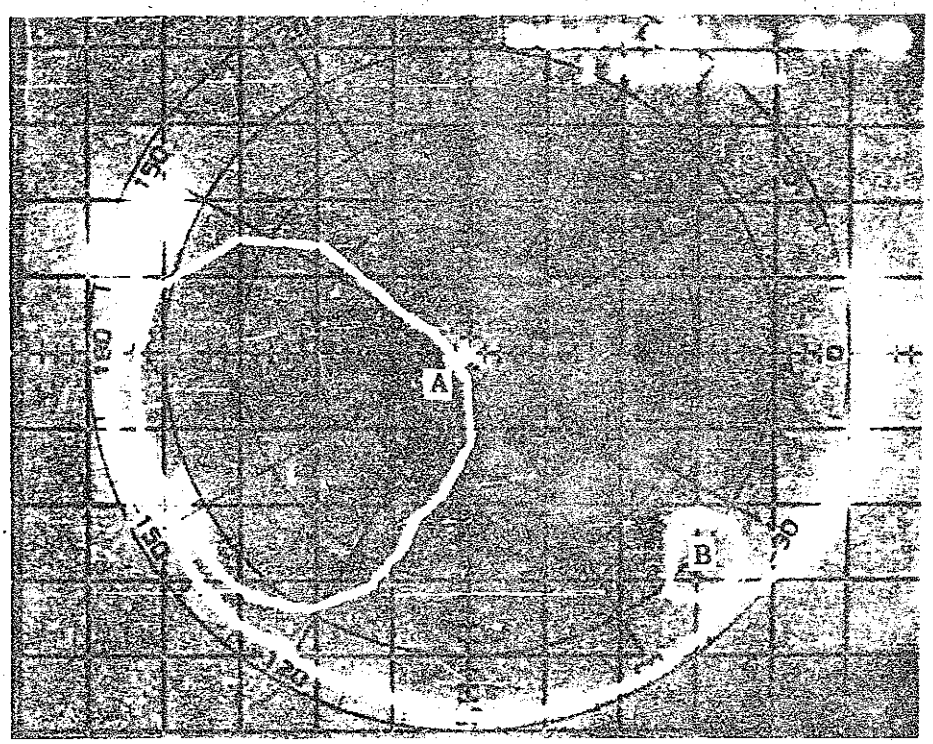

Fig.2—6.Reflection coefficient of transducer No.1 in polar coordinates with scan width f=1300MHz, A—QLW, B—QSW.

MHz is very low, which is in good agreement with the prediction. The 3 dB bandwidth of the transducer NO.1 is about 5.8%. The curve of insertion loss shown in Fig.2—7 is much similar to that of surface wave interdigital transducers[4]. Both have a periodic structure.

In time domain measurements, the pulse-echo technique has been used. The transducers are excited by a δ-pulse and echoes are observed. For lack of a sufficiently sensitive oscilloscope only the echoes of QSW for transducer No.1 are detected. They are shown in Fig.2—8(a). The details of the first echo is shown in Fig.2—8(b). From its oscillation period t=3.66ns, the frequency of the excited ultrasonic

wave can be determined which is 273MHz. This result is consistent both with the theoretical one and with the result obtained from the frequency domain measurements. The delay time measured is 1.7μs which is also compatible with the theoretical value calculated from the relation

$$\tau=2d/v_s \ , \qquad (2—33)$$

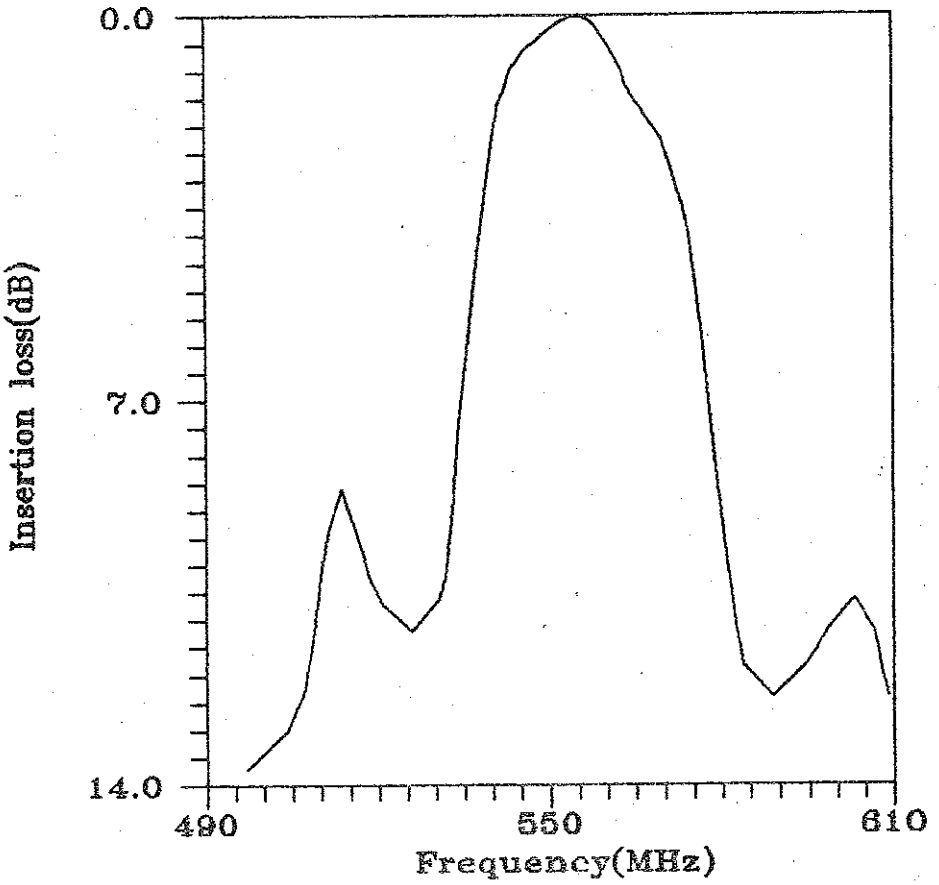

Fig.2—7.Insertion loss vs. frequency for transducer No.1.

where d is the acoustic transit distance. For the transducer NO.1, d=3.1mm. If the transmission medium is an unknown

material, then we can use Eq.(2—33) to evaluate the sound velocity of that material.

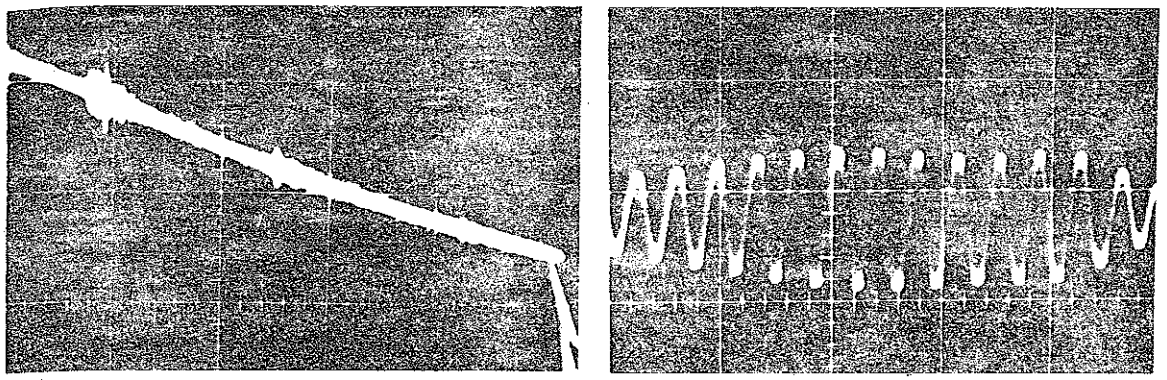

(a) (b)

Fig.2—8.(a)Oscilloscope photograph of multiple echoes produced by transducer No.1. The horizontal scale is 1μs/div.. (b)The magnified view of the first echo. Its vertical scale is 10mV/div. and the horizontal scale is 10ns/div.

§2—3.Discussions

A.Long wavelength approximation

In the previous section, in deriving the SLR, we have taken the f^1_{main} for the reference frequency. But this is not necessary. Theoretically, we can get the resonance frequency determined by the total thickness of the ASL directly from $\tan[kN(a+b)/2]\to\infty$, which is

$f^{m'}=m'v/[2N(a+b)],m'=1,3,5....$

Obviously, the $f^{m'}$ is much lower than the f^1_{main} and thus lies in the low frequency region. However, experimentally, it is not observed as Fig.2—4 indicates. This can be explained as follows.

In the low frequency region, where $\lambda >> a+b$, Eq.(2—17) can be simplified greatly. This approximation may be called long wavelength approximation as well. There are two situations of which the simplified results are quite different.

First, situation 1, we assume that apart from the condition $\lambda >> a+b$, λ is of the same order as $N(a+b)$, the total thickness of the ASL. Then Eq.(2—17) can be reduced to

$$Z=\frac{N(a+b)}{j\omega A_{12}}\left\{\frac{\varepsilon_{33}^{s}}{1-4m_1m_2k_{33}^2}\right\}^{-1}$$

$$\times\left\{1-\frac{h_{33}^2(m_1-m_2)^2}{C_{33}^{D}}\left[\frac{\varepsilon_{33}^{s}}{1-4m_1m_2k_{33}^2}\right]\frac{\tan\frac{1}{2}kN(a+b)}{\frac{1}{2}kN(a+b)}\right\}, \qquad (2—34)$$

here $m_1=a/(a+b)$, $m_2=b/(a+b)$, $k_{33}^2=h_{33}^2\varepsilon_{33}^{s}/C_{33}^{D}$ which is the electromechanical coupling coefficient.

If we let

$$\bar{h}_{33}=(m_1-m_2)h_{33},$$

$$\bar{\varepsilon}_{33}^{s}=\frac{\varepsilon_{33}^{s}}{1-4m_1m_2k_{33}^2},$$

$$\bar{k}_{33}^2=\frac{(1-4m_1m_2)k_{33}^2}{1-4m_1m_2k_{33}^2} \qquad (2—35)$$

Eq.(2—34) can be written in the form

$$Z=\frac{N(a+b)}{j\omega A_{12}\bar{\varepsilon}^{s}_{33}}\left\{1-\bar{k}^{2}_{33}\frac{\tan\frac{1}{2}kN(a+b)}{\frac{1}{2}kN(a+b)}\right\} \qquad (2—36)$$

Here $\bar{\varepsilon}^{s}_{33}$, $\bar{h}_{33}$, and $\bar{k}^{2}_{33}$ can be thought of as the average physical parameters of the crystal of ASL. Eq.(2—36) is the same as one for a resonator made of a single domain crystal with its physical parameters being $\bar{\varepsilon}^{s}_{33}$, $\bar{h}_{33}$ and $\bar{k}^{2}_{33}$ and its thickness being $N(a+b)$[5].

In this case, the structure of the ASL has no sense. The excited waves can not "see" the details of the structure. The medium acts as a homogeneous one with its parameters averaged. When $m_1=m_2$, the average piezoelectric coefficient will be zero. Thus no waves can be excited. Generally, $m_1-m_2\ll 1$, so $\bar{h}_{33}\ll h_{33}$. Therefore the waves excited will be too weak to be detected. That is why we can not see any resonance peaks in low frequency region of Fig.2—4.

But if the ASL is a compositionally modulated superlattice, the average piezoelectric coefficient may be very large. In that case,the $f^{m'}$ can be observed experimentally.

Second, situation 2, we assume that not only $\lambda\gg a+b$, but also $\lambda\gg N(a+b)$,then Eq.(2—34) can be further simplified to

$$Z=\frac{N(a+b)}{j\omega A_{12}\varepsilon^{s}_{33}}\left\{1-k^{2}_{33}\right\} \quad . \qquad (2—37)$$

This is the correct expression for the static capacitance at low frequency far from the resonance of the resonator. The resonator just acts like a capacitor. The impedance of transducers can be simplified similarly in the long wavelength regime. The average parameters deduced are the same.

The results of the average parameters in long wavelength can also be obtained by a method developed by Turik et al[11]. In their method some assumptions have been made which are equivalent to the long wavelength approximation. However, using their method, we can not distinguish the difference between situation 1 and situation 2. Here, starting from the wave equation, we have derived the expression of the average parameters very naturally. And more, we have obtained the correct expression of the static capacitance at low frequency which can not be obtained by their method.

B.The effect of echo signals on the reflection coefficient

In the case of transducers, each transducer is indium bonded to the xy plane of a single domain $LiNbO_3$ crystal separately. So the acoustic wave generated will transmit into the medium and propagate along the normal direction of the surface in the medium. When it hits the free surface of the medium, because of its being parallel to the bond surface, the wave will be echoed back and reverses its propagating direction. The acoustic impedance of the indium, the bond material, is not matched to both the transducer and

the medium. Thus the signal will propagate back and forth inside the medium. Each time the signal hits the bond surface, part of it will transmit back to the transducer and is detected by the transducer. This signal will interfere with the original one and cause the curve of the reflection coefficient rippled(see Fig.2—9). The phase difference between the two is $2\omega d/v$, where d is approximately the thickness of the medium plus half of the thickness of the ASL, v is the velocity of the sound wave in $LiNbO_3$. At certain frequencies, when the condition

$$2\omega d/v=2n\pi, \qquad (2—38)$$

is satisfied, the ripple will be at its maximum. The difference between two adjacent maximum frequencies is

$$\Delta f_1=v/2d. \qquad (2—39)$$

In some cases, if the transmitted signal is strong enough, not only may the first echo interfere with the original one, but the second echo may also interfere with the original one. By the same procedure, we get

$$\Delta f_2=v/4d. \qquad (2—40)$$

Fig.2—9 exhibits our experimental results of the transducer. The measured frequency difference Δf_{meas} is

$$\Delta f_{meas}=0.58 \text{ MHz}. \qquad (2—41)$$